Preparation of Novel 3D Graphene Networks for Supercapacitor Applications

*Xiehong Cao, Yumeng Shi, Wenhui Shi, Gang Lu, Xiao Huang, Qingyu Yan, Qichun Zhang, and Hua Zhang**

Graphene, a 2D sp^2-hybridized carbon sheet with one-atom thickness, has attracted increasing attention in recent years because of its unique structure and special properties.[1] Its high theoretical surface area (2630 $m^2 g^{-1}$) and high electrical conductivity make it an attractive material for applications in energy-storage systems.[2]

The supercapacitor is considered as a promising candidate for energy storage due to its high power performance, long life cycle, and low maintenance cost.[3] Pseudocapacitive materials, such as transition metal oxides, are being explored for use in supercapacitors with a large specific capacitance and high energy density.[4] However, pseudocapacitors often suffer from the low rate capability and poor stability, because the active materials are usually insulating or semiconducting, which hinders the fast electron transport required for high charge/discharge rates.

As an ideal matrix, graphene is commonly used for growth of functional nanomaterials.[1a,2c,5] Recently, nanocomposites made by graphene and transition metal oxides have attracted wide attention in the field of supercapacitors due to their synergetic effect, arising from the combination of the redox reaction of metal oxides with the high surface area/conductivity of graphene, to improve the electrochemical performance.[6] It has been reported that the electrochemical performance of these composites is highly dependent on the quality and conductivity of graphene.[6c]

X. Cao,[+] Dr. Y. Shi,[+] W. Shi,[+] G. Lu, X. Huang, Prof. Q. Yan, Prof. Q. Zhang, Prof. H. Zhang
School of Materials Science and Engineering
Nanyang Technological University
50 Nanyang Avenue, Singapore 639798, Singapore
Tel: (+65) 67905175; Fax: (+65) 67909081
Website: http://www.ntu.edu.sg/home/hzhang
E-mail: hzhang@ntu.edu.sg

W. Shi, Prof. Q. Yan
Energy Research Institute
Nanyang Technological University
637459, Singapore

Prof. Q. Yan
TUM CREATE Centre for Electromobility
Nanyang Technological University
637459, Singapore

[+] These authors contributed equally to this work.

DOI: 10.1002/smll.201100990

Normally, the chemically exfoliated graphene oxide (GO) is used as a synthetic template for graphene-based composites.[1,7] Although GO is readily produced in large quantities,[8] it is poorly conductive due to the surface defects and oxygen-containing groups introduced during the oxidation process of graphite. Even after GO is reduced, the reduced graphene oxide (rGO) is still less conductive than the pristine graphene.[9] In addition, the hydrophobic rGO sheets are easy to aggregate and restack, due to the partial removal of hydrophilic functional groups after the reduction of GO.

Chemical vapor deposition (CVD) is an alternative method to produce graphene with high conductivity comparable to the pristine graphene,[10] which would facilitate the fast electron transport between the active materials and current collectors in supercapacitors.[6a,6c] However, the CVD-synthesized graphene is commonly grown on a flat metal foil or thin film;[10] thus its application in energy storage is greatly limited due to the low-yield production. In addition, the conventional synthesis of graphene-based composites is mostly based on wet-chemical methods. This makes CVD-synthesized graphene, which contains no functional groups, less applicable in the synthesis of graphene-based composites, due to its extremely low solubility in commonly used solvents.

In this Communication, we report the preparation of novel 3D graphene networks by using Ni foam as a sacrificial template in a facile CVD process with ethanol as the carbon source, referred to as ethanol-CVD. It provides a good method to scale up the CVD synthesis of graphene. Moreover, we demonstrate that the 3D graphene networks are excellent templates for the construction of graphene/metal oxide composites, which can be used as supercapacitor electrodes. As a proof of concept, nickel oxide (NiO) has been electrochemically deposited on the 3D graphene networks. The unique 3D porous structure of the graphene network with a large specific surface area allows the rapid access of electrolyte ions to the NiO surface. The direct synthesis of graphene on current collector of Ni foam by CVD affords an effective electrical contact for fast charge transfer from active materials to current collectors via the underlying 3D graphene network. Consequently, the obtained NiO/graphene composite exhibits a high specific capacitance of ≈816 F g^{-1} at a scan rate of 5 mV s^{-1} and a stable cycling performance without any decrease of its specific capacitance after 2000 cycles.

Scheme 1 illustrates the fabrication of 3D graphene networks on Ni foam by ethanol-CVD. Compared to other CVD

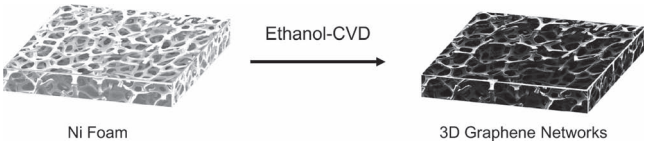

Scheme 1. Schematic illustration of the synthesis of 3D graphene networks on Ni foam by ethanol-CVD.

processes, which use vacuum and explosive carbon sources (e.g. CH_4),[10] ethanol is safe and cheap. After the growth of graphene, the color of the Ni foam changed from shiny white to dark gray (**Figure 1**a). Moreover, after removal of the Ni foam, ≈0.1 g graphene was obtained in a single CVD process (Figure 1b). In principle, the production can be easily scaled up by using a larger CVD chamber, which is essential for practical applications.

Figure 1c shows a scanning electron microscopy (SEM) image of 3D graphene networks grown on Ni foam after the CVD process. Ripples and wrinkles of graphene were observed on the surface of Ni foam (Figure S1a in Supporting Information (SI)), which arises from the different thermal expansion coefficients of Ni and graphene.[10b] Those wrinkles can provide graphene with a large surface area and good mechanical properties.[10b] After removal of the Ni template, the graphene sheets replicate the 3D network and porous structure of Ni foam well without collapse (Figure 1b,d and Figure S1c in SI). The intrinsic grains and wrinkles of graphene sheets (Figure S1b in SI) were well remained without any observable crack or break, indicating a continuous network of graphene. Figure 1e

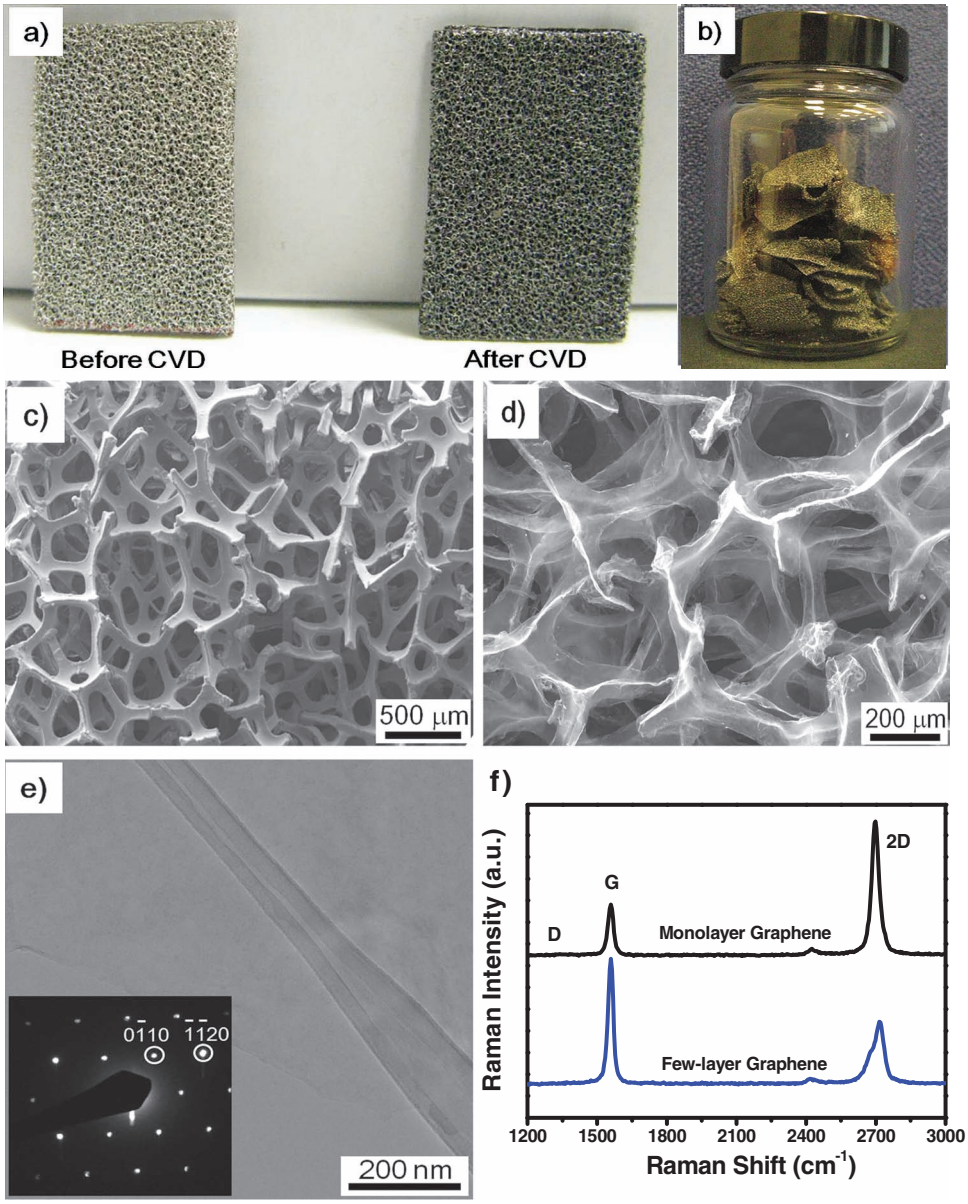

Figure 1. Photographs of a) Ni foam before and after the growth of graphene, and b) ≈0.1 g 3D graphene networks obtained in a single CVD process after removal of the Ni foam. SEM images of c) 3D graphene networks grown on Ni foam after CVD, and d) 3D graphene networks after removal of Ni foam. e) TEM image of a graphene sheet. Inset: SAED pattern of graphene sheet. f) Raman spectra of 3D graphene networks.

small NANO MICRO

shows the transmission electron microscopy (TEM) image of a graphene sheet. The selected area electron diffraction (SAED) pattern (inset of Figure 1e) gives reflection spots arranged in a typical hexagonal pattern,[11] which suggests the formation of graphene after CVD.

The 3D graphene networks were also characterized by Raman spectroscopy. Typical Raman spectra (Figure 1f) indicate the 3D graphene networks contain mono- to few-layer graphene, exhibiting two distinct peaks at ≈1559 cm^{-1} (G-band) and ≈2699 cm^{-1} (2D-band).[12] Since the D-band (usually at ≈1300 cm^{-1}) is attributable to the disordered carbon in graphene, and its intensity provides information about the density of defects in the as-grown graphene film,[13] it is worth mentioning that the D-bands of 3D graphene networks are extremely feeble (Figure 1f), indicating the good quality of graphene grown by ethanol-CVD.

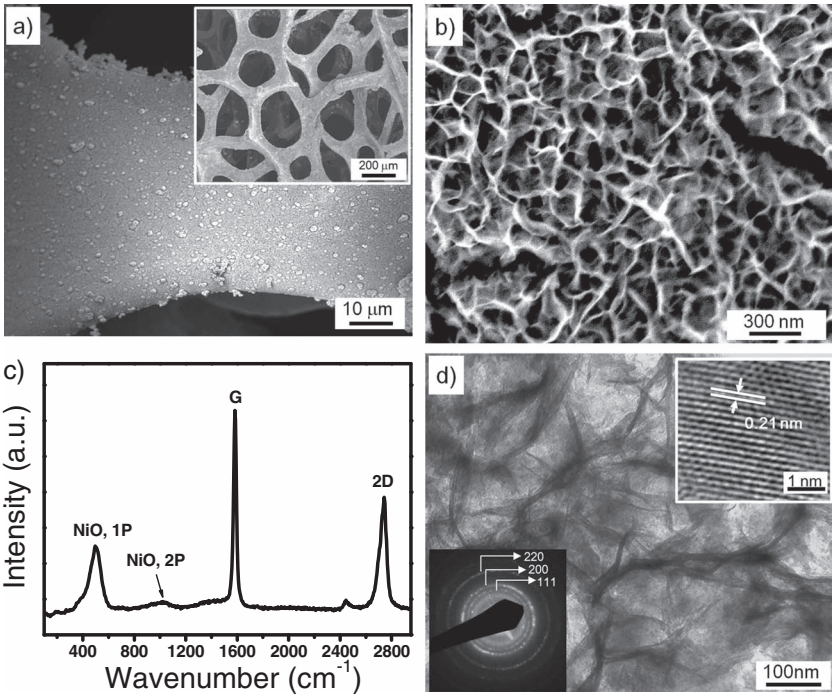

Figure 2. SEM image of a) a branch of 3D graphene network coated with NiO. Inset: NiO film deposited on a 3D graphene network. b) Magnified SEM image of NiO/graphene composites in (a). c) Raman spectrum of NiO/graphene composites. d) TEM image of NiO film deposited on 3D graphene network. Inset: (Top) HRTEM image and (Bottom) SAED pattern of NiO.

As a proof of concept, the 3D graphene networks are used as templates to construct graphene/metal oxide composites for supercapacitor applications. Nickel oxide (NiO) is a promising material for supercapacitors,[4b,14] because of its high specific capacitance, well-accepted redox behavior, and low cost. Hereby, the porous NiO film, as an example, was deposited on the 3D graphene network by the potentiostatic electrodeposition method.[14b] The conventional electrode fabrication method requires the polymeric binders to stick powder samples to current collectors such as Ni foam, which decrease the conductivity of the electrode, leading to a large contact resistance between the active materials and the current collector. Since the 3D graphene network synthesized in our experiment is precipitated onto the Ni foam via CVD at a high temperature, the graphene films possess effective electrical contact with the Ni foam. Thus, the as-prepared NiO/graphene composites on Ni foam can be used for electrochemical testing directly, without any further treatment.

Figure 2a shows an SEM image of 3D graphene network coated with a layer of NiO. The NiO film exhibits petal-like and porous morphology (Figure 2b). The resulting NiO/graphene composite was also characterized by Raman spectroscopy and TEM. As shown in Figure 2c, the NiO/graphene composite exhibits two additional Raman peaks compared to 3D graphene networks (Figure 1f), i.e., a sharp peak at ≈496 cm^{-1} and a broad one at ≈1024 cm^{-1}, which can be assigned to first- (1P) and second-order phonon (2P) scattering, respectively, in NiO.[15] Raman mapping of the 1P band (246–633 cm^{-1}) shows the signal of NiO (Figure S2 in SI), suggesting the dense and uniform coating of NiO on 3D graphene networks, which is in agreement with the SEM observations (Figure 2a).

Figure 2d shows a typical TEM image of folded NiO film deposited on 3D graphene network. The HRTEM image (top inset in Figure 2d) shows a lattice spacing of 0.21 nm, which can be assigned to the interplanar distance of the (200) planes of NiO with the face-centered cubic (fcc) structure. The SAED pattern (bottom inset in Figure 2d) reveals three distinct diffraction rings, corresponding to the (111), (200), and (220) planes of fcc NiO (Joint Committee for Powder Diffraction Standards 78-0643).[16]

The electrochemical performance of the NiO/graphene composite electrode was analyzed using cyclic voltammetry (CV) and galvanostatic charge–discharge measurements in 3 mol L^{-1} KOH aqueous solution in the potential window from 0 to 0.5 V. **Figure 3**a shows the CV response of NiO/graphene at different scan rate ranging from 5 to 40 mV s^{-1}. A pair of cathodic and anodic peaks was observed, which corresponds to the reversible reactions of $Ni^{II} \leftrightarrow Ni^{III}$.[14a] The well-accepted surface Faradaic reaction of nickel oxide is expressed in the equation: $NiO + OH^- \leftrightarrow NiOOH + e^-$.[14a]

With the increase of scan rate, the current response increased accordingly, while no significant change in the shape of CV curve was observed, indicating the good rate property of the NiO/graphene composite electrode. Based on the equation, $C = \frac{\int Id\,V}{v\,m\,V}$,[17] where C is the specific capacitance based on the mass of electroactive material (F g^{-1}), I is the response current (A), v is the potential scan rate (V s^{-1}), m is the mass of the electroactive materials in the electrodes (g) and V is the potential (V); the specific capacitance of NiO/graphene composite calculated from the CV curve is 816 and 573 F g^{-1} at scan rates of 5 and 40 mV s^{-1}, respectively (Figure 3b). Figure 3c shows the galvanostatic discharge curves of the NiO/graphene composite at a broad current-density range from 1.4 to 20 A g^{-1}. At a discharge current density of 1.4 A g^{-1},

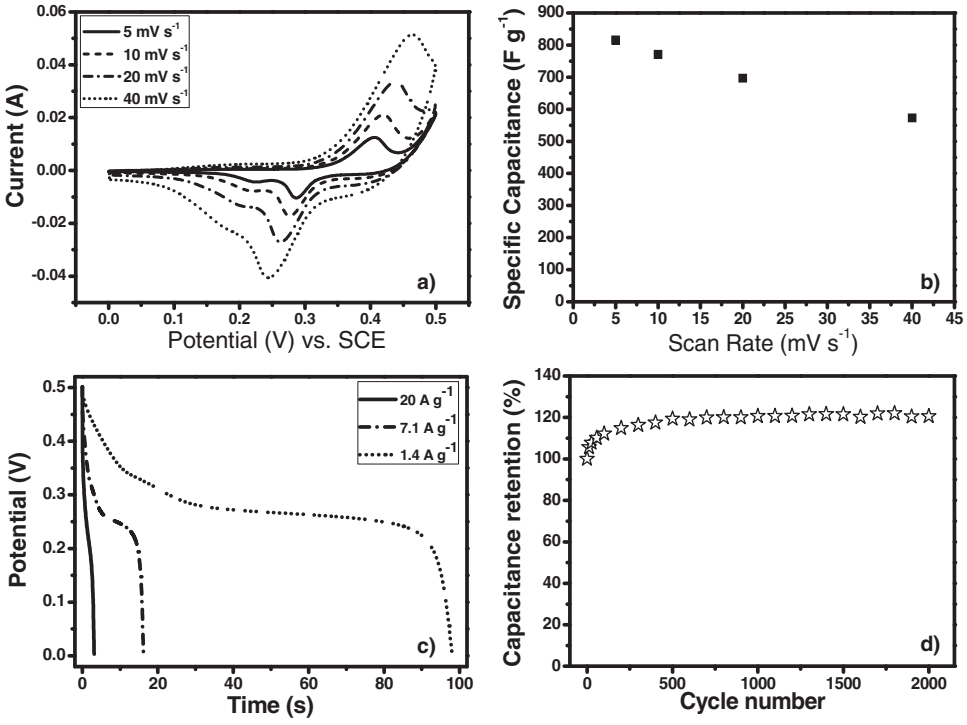

Figure 3. Electrochemical performance of NiO/graphene composites. a) Cyclic voltammetry curves measured at scan rate of 5, 10, 20, and 40 mV s^{-1}. b) Specific capacitance as a function of scan rate. c) Galvanostatic discharge curves measured at current density of 1.4, 7.1, and 20 A g^{-1}. d) The cycling performance measured at a scan rate of 80 mV s^{-1} in 3 mol L^{-1} KOH with potential range from 0–0.5 V.

the NiO/graphene shows a specific capacitance of as high as 745 F g^{-1}.

The cycling performance of NiO/graphene composite at a scan rate of 80 mV s^{-1} is shown in Figure 3d. The specific capacitance increased of about 15% during the first 200 cycles, which is possibly due to the activation process that allows the trapped ions to gradually diffuse out.[14a] Importantly, there is no obvious capacitance drop over 2000 cycles, demonstrating the excellent electrochemical stability of the NiO/graphene composite.

As a comparison, NiO was electrochemically deposited directly onto the Ni foam, referred to as NiO/Ni foam, which exhibited a specific capacitance of 305 F g^{-1} at a scan rate of 5 mV s^{-1} (Figure S3 in SI), much lower than that obtained from the NiO/graphene composite (Figure 3b). Such superior supercapacitor performance of the NiO/graphene composite can be attributed to the following reasons. First, graphene is directly precipitated on the Ni foam, thus the graphene sheets have a good electrical contact with the current collector (Ni foam). Second, the electrochemical deposition method renders the as-deposited NiO in close contact with the 3D graphene network, leading to rapid charge transport from NiO to current collector via the network. Third, the 3D conductive graphene network, with its porous structure (Figure 1d), guarantees the large surface area of deposited NiO film, which directly contacts with electrolyte, resulting in fast and easy access of electrolyte ions to the surface of NiO, reducing the diffusion resistance of electrolyte.

The significantly improved charge transfer and faster ion-transport behavior of NiO/graphene composite was further confirmed by the electrochemical impedance spectroscopy (EIS) analysis. As shown in the Nyquist plot in Figure S4 (SI), the NiO/graphene composite electrode exhibits a smaller radius semi-circle in the high-frequency region as compared to the NiO/Ni foam electrode, which indicates a good electrical contact in the electrode.[18] In the low-frequency region, the plot of the NiO/graphene composite electrode shows a higher slope, suggesting that ion diffusion is fast enough to catch up with the change of frequency,[19] which might result from the unique 3D structure of the NiO/graphene composite.

In summary, a novel graphene material, i.e., a 3D graphene network, is synthesized by the ethanol-CVD method. The 3D graphene network, made of high-quality graphene films, can be produced on a large scale. It is demonstrated that the 3D graphene network can serve as a good platform to construct graphene/metal oxide composites for surpercapacitor applications. The NiO/graphene composite electrode exhibits a high specific capacitance of 816 F g^{-1} at 5 mV s^{-1} and a good rate capability. In principle, other metal oxides with high specific capacitance, such as RuO_2,[4c,20] and MnO_2,[4a,6d,21] are also feasible to be incorporated into the 3D graphene network. Our method offers a new way to fabricate graphene-based composite materials. We believe that the versatile composites based on 3D graphene networks and metal oxides would have promising applications in various energy-storage devices.

Experimental Section

Growth of 3D Graphene Networks by CVD: Nickel foams (density of ≈380 g m^{-2} and thickness of ≈1.6 mm, purchased from Changsha

NANO MICRO small

lyrun new material Co. Ltd, China) were placed in the centre of a quartz tube furnace and annealed at 1000 °C for 5 min under the gas flow of Ar (200 sccm) and H_2 (40 sccm), in order to reduce the oxide layers of Ni foam. Ethanol was then bubbled into the tube by Ar flow under ambient pressure at 1000 °C. The concentration of ethanol can be adjusted by the flow rate of Ar. After 10 min, the quartz tube was taken out of furnace, and then cooled down to room temperature under the protection of Ar (200 sccm) and H_2 (40 sccm) at a cooling rate of ≈100 °C min^{-1}. After growth of graphene, the color of Ni foam changed from shiny white to dark gray (Figure 1a).

To remove the Ni foam, the 3D graphene network was first coated with poly(methyl methacrylate) (PMMA) by immersing it in the PMMA solution (4.5 wt% PMMA with molecular weight ≈996 000 in anisole) for several seconds, and then dried at 90 °C for 1 h, followed by immersing into an etchant solution containing 1 mol L^{-1} $FeCl_3$ and 2 mol L^{-1} HCl at 50 °C. After removal of Ni foam, the PMMA coated on 3D graphene network was removed by hot acetone vapor followed by annealing at 450 °C under Ar (200 sccm) and H_2 (40 sccm).

Preparation of NiO Film on 3D Graphene Network: The electrochemical deposition of NiO was performed using an electrochemical workstation (CHI600C, CH Instrument Inc., USA).[14b] The 3D graphene network electrode, a Pt wire and a Ag/AgCl (sat. KCl) electrode were used as the working, counter, and reference electrode, respectively. The electrolyte contains 0.2 mol L^{-1} $Ni(NO_3)_2{\cdot}6H_2O$ and 0.2 mol L^{-1} hexamethylenetetramine ($C_6H_{12}N_4$). Firstly, $Ni(OH)_2$ was deposited on the 3D graphene network electrode by a potentiostatic process at -0.5 V at 70 °C. Then the electrode was rinsed with DI water, followed by drying with N_2. The obtained sample was annealed under Ar at 300 °C for 1 h to form crystalline NiO film. The heating and cooling rate was 5 °C min^{-1}.

Sample Characterization: Field emission scanning electron microscopy (FESEM, Model JSM-7600F, JEOL Ltd., Tokyo, Japan) and transmission electron microscopy (TEM, Model JSM-2100 and JSM-2010, JEOL Ltd., Tokyo, Japan) were used to characterize the samples. Raman spectra were collected with a WITEC CRM200 Raman System (488 nm laser, 2.54 eV, WITec, Germany). To prepare the TEM samples, the NiO/graphene composite on Ni foam was first sonicated in ethanol for 1 min, and then a droplet of the obtained suspension was dropped onto a TEM grid, followed by naturally drying at ambient conditions.

Electrochemical Measurements: All the electrochemical measurements were performed in a conventional three-electrode system. 3 mol L^{-1} KOH aqueous solution was used as the electrolyte. Cyclic voltammetry (CV) and galvanostatic charge/discharge tests were performed in Solartron analytical equipment (Model 1470E, AMETEK, UK).

Supporting Information

Supporting Information is available from the Wiley Online Library or from the author.

Acknowledgements

*This work was supported by AcRF Tier 2 (ARC 10/10, No. MOE2010-T2-1-060) from MOE, CRP (NRF-CRP2-2007-01) from NRF, CREATE program (Nanomaterials for Energy and Water Management) from NRF and New Initiative Fund FY 2010 (M58120031) from NTU in Singapore. Q.Y. thanks the support from AcRF Tier 1 RG 31/08 of MOE (Singapore), NRF2009EWT-CERP001-026 (Singapore), Singapore Ministry of Education (MOE2010-T2-1-017), A*STAR SERC grant 1021700144 and Singapore MPA 23/04.15.03 RDP 009/10/102 and MPA 23/04.15.03 RDP 020/10/113 grant.*

[1] a) X. Huang, Z. Yin, S. Wu, X. Qi, Q. He, Q. Zhang, Q. Yan, F. Boey, H. Zhang, *Small* **2011**, *7*, 1876; b) X. Huang, X. Y. Qi, F. Boey, H. Zhang, *Chem. Soc. Rev.* DOI: 10.1039/C1CS15078B.

[2] a) M. D. Stoller, S. Park, Y. Zhu, J. An, R. S. Ruoff, *Nano Lett.* **2008**, *8*, 3498; b) L. L. Zhang, R. Zhou, X. S. Zhao, *J. Mater. Chem.* **2010**, *20*, 5983; c) Y. Wang, Z. Q. Shi, Y. Huang, Y. F. Ma, C. Y. Wang, M. M. Chen, Y. S. Chen, *J. Phys. Chem. C* **2009**, *113*, 13103; d) C. G. Liu, Z. N. Yu, D. Neff, A. Zhamu, B. Z. Jang, *Nano Lett.* **2010**, *10*, 4863.

[3] a) A. S. Arico, P. Bruce, B. Scrosati, J.-M. Tarascon, W. van Schalkwijk, *Nat. Mater.* **2005**, *4*, 366; b) P. Simon, Y. Gogotsi, *Nat. Mater.* **2008**, *7*, 845; c) L. L. Zhang, X. S. Zhao, *Chem. Soc. Rev.* **2009**, *38*, 2520.

[4] a) R. Ma, Y. Bando, L. Zhang, T. Sasaki, *Adv. Mater.* **2004**, *16*, 918; b) C. Yuan, X. Zhang, L. Su, B. Gao, L. Shen, *J. Mater. Chem.* **2009**, *19*, 5772; c) R.-R. Bi, X.-L. Wu, F.-F. Cao, L.-Y. Jiang, Y.-G. Guo, L.-J. Wan, *J. Phys. Chem. C* **2010**, *114*, 2448; d) Y. Wang, I. Zhitomirsky, *Langmuir* **2009**, *25*, 9684.

[5] a) Q. Wu, Y. X. Xu, Z. Y. Yao, A. R. Liu, G. Q. Shi, *ACS Nano* **2010**, *4*, 1963; b) D. S. Yu, L. M. Dai, *J. Phys. Chem. Lett.* **2010**, *1*, 467; c) Z. Fan, J. Yan, L. Zhi, Q. Zhang, T. Wei, J. Feng, M. Zhang, W. Qian, F. Wei, *Adv. Mater.* **2010**, *22*, 3723.

[6] a) W. Shi, J. Zhu, D. H. Sim, Y. Y. Tay, Z. Lu, X. Zhang, Y. Sharma, M. Srinivasan, H. Zhang, H. H. Hng, Q. Yan, *J. Mater. Chem.* **2011**, *21*, 3422; b) J. Zhu, T. Zhu, X. Zhou, Y. Zhang, X. W. Lou, X. Chen, H. Zhang, H. H. Hng, Q. Yan, *Nanoscale* **2011**, *3*, 1084; c) H. Wang, H. S. Casalongue, Y. Liang, H. Dai, *J. Am. Chem. Soc.* **2010**, *132*, 7472; d) S. Chen, J. Zhu, X. Wu, Q. Han, X. Wang, *ACS Nano* **2010**, *4*, 2822.

[7] a) X. Huang, S. Li, Y. Huang, S. Wu, X. Zhou, S. Li, C. L. Gan, F. Boey, C. A. Mirkin, H. Zhang, *Nat. Commun.* **2011**, *2*, 292; b) X. Qi, K.-Y. Pu, H. Li, X. Zhou, S. Wu, Q.-L. Fan, B. Liu, F. Boey, W. Huang, H. Zhang, *Angew. Chem. Int. Ed.* **2010**, *49*, 9426; c) X. Cao, Q. He, W. Shi, B. Li, Z. Zeng, Y. Shi, Q. Yan, H. Zhang, *Small* **2011**, *7*, 1199; d) X. Qi, K.-Y. Pu, X. Zhou, H. Li, B. Liu, F. Boey, W. Huang, H. Zhang, *Small* **2010**, *6*, 663; e) Z. Yin, S. Wu, X. Zhou, X. Huang, Q. Zhang, F. Boey, H. Zhang, *Small* **2010**, *6*, 307; f) X. Huang, X. Zhou, S. Wu, Y. Wei, X. Qi, J. Zhang, F. Boey, H. Zhang, *Small* **2010**, *6*, 513; g) X. Zhou, X. Huang, X. Qi, S. Wu, C. Xue, F. Y. C. Boey, Q. Yan, P. Chen, H. Zhang, *J. Phys. Chem. C* **2009**, *113*, 10842; h) H. Wang, J. T. Robinson, G. Diankov, H. Dai, *J. Am. Chem. Soc.* **2010**, *132*, 3270; i) S. Stankovich, D. A. Dikin, G. H. B. Dommett, K. M. Kohlhaas, E. J. Zimney, E. A. Stach, R. D. Piner, S. T. Nguyen, R. S. Ruoff, *Nature* **2006**, *442*, 282.

[8] a) X. Zhou, G. Lu, X. Qi, S. Wu, H. Li, F. Boey, H. Zhang, *J. Phys. Chem. C* **2009**, *113*, 19119; b) D. Li, M. B. Muller, S. Gilje, R. B. Kaner, G. G. Wallace, *Nat. Nanotechnol.* **2008**, *3*, 101; c) J. Luo, L. J. Cote, V. C. Tung, A. T. L. Tan, P. E. Goins, J. Wu, J. Huang, *J. Am. Chem. Soc.* **2010**, *132*, 17667.

[9] a) Z. Yin, S. Sun, T. Salim, S. Wu, X. Huang, Q. He, Y. M. Lam, H. Zhang, *ACS Nano* **2010**, *4*, 5263; b) Q. He, S. Wu, S. Gao, X. Cao, Z. Yin, H. Li, P. Chen, H. Zhang, *ACS Nano* **2011**, *5*, 5038; c) Q. He, H. G. Sudibya, Z. Yin, S. Wu, H. Li, F. Boey, W. Huang, P. Chen, H. Zhang, *ACS Nano* **2010**, *4*, 3201; d) H. Wang, J. T. Robinson, X. Li, H. Dai, *J. Am. Chem. Soc.* **2009**, *131*, 991031;

e) X. Li, G. Zhang, X. Bai, X. Sun, X. Wang, E. Wang, H. Dai, *Nat. Nanotechnol.* **2008**, *3*, 538.
[10] a) X. Li, W. Cai, J. An, S. Kim, J. Nah, D. Yang, R. Piner, A. Velamakanni, I. Jung, E. Tutuc, S. K. Banerjee, L. Colombo, R. S. Ruoff, *Science* **2009**, *324*, 1312; b) K. S. Kim, Y. Zhao, H. Jang, S. Y. Lee, J. M. Kim, K. S. Kim, J.-H. Ahn, P. Kim, J.-Y. Choi, B. H. Hong, *Nature* **2009**, *457*, 706.
[11] J. C. Meyer, A. K. Geim, M. I. Katsnelson, K. S. Novoselov, T. J. Booth, S. Roth, *Nature* **2007**, *446*, 60.
[12] A. C. Ferrari, J. C. Meyer, V. Scardaci, C. Casiraghi, M. Lazzeri, F. Mauri, S. Piscanec, D. Jiang, K. S. Novoselov, S. Roth, A. K. Geim, *Phys. Rev. Lett.* **2006**, *97*, 187401.
[13] a) M. S. Dresselhaus, A. Jorio, M. Hofmann, G. Dresselhaus, R. Saito, *Nano Lett.* **2010**, *10*, 751; b) A. C. Ferrari, *Solid State Commun.* **2007**, *143*, 47.
[14] X. Zhang, W. Shi, J. Zhu, W. Zhao, J. Ma, S. Mhaisalkar, T. Maria, Y. Yang, H. Zhang, H. Hng, Q. Yan, *Nano Res.* **2010**, *3*, 643; b) Y. Y. Xi, D. Li, A. B. Djurisic, M. H. Xie, K. Y. K. Man, W. K. Chan, *Electrochem. Solid-State Lett.* **2008**, *11*, D56.
[15] a) R. E. Dietz, G. I. Parisot, A. E. Meixner, *Phys. Rev. B* **1971**, *4*, 2302; b) R. E. Dietz, W. F. Brinkman, A. E. Meixner, H. J. Guggenheim, *Phys. Rev. Lett.* **1971**, *27*, 814.
[16] X. Liu, G. Qiu, Z. Wang, X. Li, *Nanotechnology* **2005**, *16*, 1400.
[17] H. Wang, Q. Hao, X. Yang, L. Lu, X. Wang, *Nanoscale* **2010**, *2*, 2164.
[18] L. L. Zhang, S. Zhao, X. N. Tian, X. S. Zhao, *Langmuir* **2010**, *26*, 17624.
[19] Y. Sun, Q. Wu, Y. Xu, H. Bai, C. Li, G. Shi, *J. Mater. Chem.* **2011**, *21*, 7154.
[20] Z. S. Wu, D. W. Wang, W. Ren, J. Zhao, G. Zhou, F. Li, H. M. Cheng, *Adv. Funct. Mater.* **2010**, *20*, 3595.
[21] Z.-S. Wu, W. Ren, D.-W. Wang, F. Li, B. Liu, H.-M. Cheng, *ACS Nano* **2010**, *4*, 5835.

Received: May 22, 2011
Published online: September 20, 2011